Elastic contour mapping for the estimation of abrupt shape deformations

Ignacio Cuiral-Zueco and Gonzalo López-Nicolás

Instituto de Investigación en Ingeniería de Aragón, Universidad de Zaragoza, Spain
ignaciocuiral@unizar.es, gonlopez@unizar.es

Abstract. Estimating object deformations is important in various industrial applications, such as material testing or object shape control. However, existing methods assume smooth or gradual deformations and thus face a significant challenge when it comes to sudden changes in an object's shape. In this paper, we propose a novel approach using our FMM-based contour mapping framework to estimate the deformation mesh of texture-less objects that experience abrupt shape changes. By analysing the contour's geometry, we compute a map between the contours of consecutive deformation states, which we use as input to update the deformation mesh. Our experiments and comparisons demonstrate the effectiveness of our method in handling abrupt deformations and accurately estimating the object's deformation mesh.

Keywords: deformable object perception, deformation mesh estimation

1 Introduction

Estimating the deformation state of objects [1] is important in various industrial processes [2,3] as it has various practical applications such as identifying the object's behaviour (useful in material testing), computing a deformation model for shape control [4] (beneficial in robotics and automation) or performing more specific tasks (such as cloth smoothing [5]). Deformation meshes provide a discrete approximation of the continuous deformation behaviour of objects and thus characterise the object's deformation state. Current methods in the literature typically rely on matching visual features between iterations to update the object's mesh nodes (e.g., [4, 6, 7]). However, in cases where the visual texture of the object is not distinctive, such as objects without texture or with repetitive patterns, obtaining an adequate estimation of the object's deformation state becomes a challenge. In our related work [8], we also exploit the elastic FMM (Fast Marching Method) based contour mapping method for identifying deformations. The framework in [8] seeks object-compliant shape control, that is, it allows to achieve shape control by also considering and reducing the amount of deformation the object undergoes during the control process. However, in such framework we only consider smooth and slow deformations. Therefore, obtaining an adequate estimation of the object's deformation state when sudden shape changes take place and without relying on its visual texture presents a challenge.

Building on our earlier research [9], we propose a new method in this paper that tackles this problem.

In [9], we introduced a method for contour mapping that maximises the similarity between geometric characteristics of matched contours using our proposed multi-scale Laplacian descriptors and the FMM. This method is particularly interesting for robust estimation of deformations as it can handle non-isometric mappings (diffeomorphisms) between contours. In the case of small and smooth deformations, a homogeneous contour mapping method can be used to estimate the object's deformation between consecutive states without causing significant errors or drift. However, when object states change abruptly due to fast deformations or low sampling rates, assuming isometric deformations may result in inaccurate estimations of the actual deformation process. Focusing on this problem, in this paper we apply the mapping method from [9] to estimate the deformation mesh of the object, even when consecutively measured states present abrupt changes. This paper collects our work presented at the 3rd Workshop on Representing and Manipulating Deformable Objects, organised in the International Conference on Robotics and Automation (ICRA) 2023.

This paper is organised as follows: section 2.1 provides a summary of the elastic mapping method presented in [9]. Section 2.2 details the proposed framework, which is the main contribution of this paper. The experimental results are presented in Section 3, followed by a final discussion in Section 4.

2   Mesh estimation method

2.1   FMM-based contour mapping

For completeness, in this section we summarise the elastic mapping method presented in [9]. The method takes as input two contours that are uniformly sampled and parameterised with parameters $\theta, \bar{\theta}$. We begin by computing the multi-scale Laplacian descriptors for both contours (as detailed in Section III.A. of [9]). These descriptors are computed at each point along the contour in the local reference frame, ensuring descriptor invariance to rigid transformations applied to the contours. Furthermore, the multi-scale nature of the descriptors enables comparison of local and larger size geometric features. After computing both descriptors, they are compared by generating a similarity surface denoted by $F(\theta, \bar{\theta}) \in \mathbb{R}^2$, where $F(\theta, \bar{\theta})$ represents how similar (in geometric terms) the respective neighbouring regions of points θ and $\bar{\theta}$ are.

The FMM [10] is applied to $F(\theta, \bar{\theta})$ to compute path $P \in \mathbb{R}^2$. This path, defined on surface $F(\theta, \bar{\theta})$ as $P = (\theta, \Pi(\theta))$, generates the coordinate pairs (or contour map) $\Pi(\theta) = \bar{\theta}$ that accumulate the lowest comparison cost when *travelling* along surface $F(\theta, \bar{\theta})$ (see Fig. 1). Path P is usually referred to as the shortest path; the integral of the comparison cost $1/F(\theta, \bar{\theta})$ along P (i.e., $\int 1/F(\theta, \Pi(\theta))\mathrm{d}\theta$) represents the shortest *shape distance* between two compared contours according to our descriptors. Contour point matches can be directly obtained from the shortest path coordinates by setting a point's parameter θ as
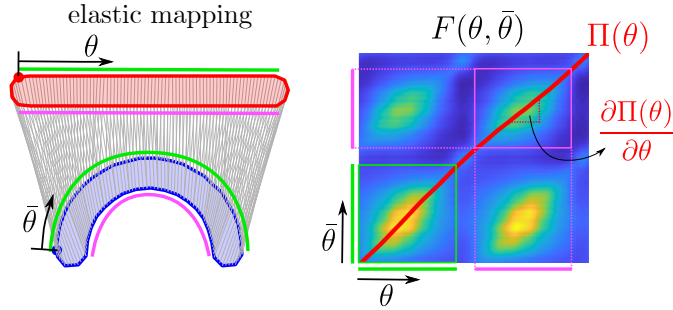
Fig. 1. Shape comparison example that shows the importance of using an elastic mapping method to identify where deformations take place. On the left, two deformation states of an object are represented by its contour: the red contour constitutes the at-rest state and the blue contour the deformed state after a bending process occurred. The green and purple lines serve as reference to identify the contour's segments on the axes of the similarity surface $F(\theta, \bar{\theta})$. Note how the green segment barely changes its length as it constitutes the outer arch, whereas the purple segment is shortened as the inner arch constitues a compressed region of the object. This is reflected on the slope of path P, constituted by $\partial \Pi(\theta)/\partial \theta$: the green segments, as the contour length does not change on that region, are homogeneously mapped. That is, the mapping's slope is approximately $\partial \Pi(\theta)/\partial \theta \approx 1$. However, the purple segments are mapped after a compressing process that results in a slight slope of $\partial \Pi(\theta)/\partial \theta < 1$.

input to the path coordinates $(\theta, \Pi(\theta) = \bar{\theta})$. In a more intuitive manner: the FMM defines a mapping cost surface and a least-resistance travelling path along such surface. The cost surface is defined by comparing each point of the current contour with every point of the target contour and determining how different they are (according to our descriptors). The accumulated cost obtained from the mapping path as it travels through the cost surface leads to the overall cost of contour mapping.

2.2   Mesh estimation for abrupt deformations

Figure 2 presents the proposed vision-based method for estimating the deformation mesh of predominantly planar texture-less objects that present abrupt (sudden) deformations. The method processes RGB images captured by a camera to perform a colour-based object segmentation (in the CieLAB colour space) and to extract the object's contour (using α-shape contour extraction). At the beginning of the process ($k = 1$, being $k \in \mathbb{N}$ the iteration number), the initial mesh is generated from the contour information using DistMesh [11] under the assumption that the object is at rest. In each iteration, the mesh is updated using object contours extracted from incoming frames. The FMM-based contour mapping compares consecutively retrieved contours to obtain contour point matches, which are used as input for the mesh simulation process. This enables updating positions of nodes that are not part of the contour. A variety of mesh-based
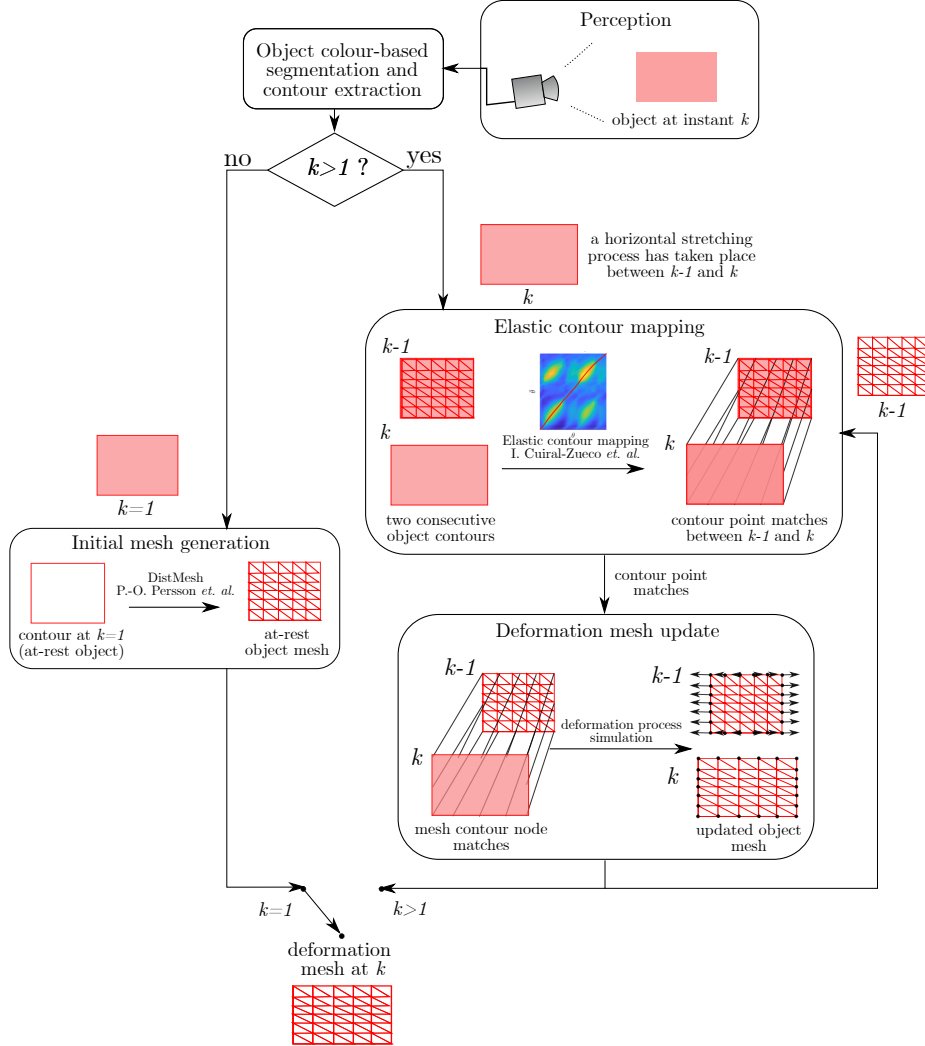
Fig. 2. Flowchart of the proposed method, where $k \in \mathbb{N}$ is used to refer to time iterations. Assuming that the object begins in at-rest state, the initial mesh is generated at the beginning of the process ($k = 1$) using DistMesh [11]. In each iteration, the mesh is updated using the object's contour from incoming frames ($k > 1$). Contour mapping based on the FMM compares consecutively retrieved contours, obtaining contour point matches, which are used as input for the mesh simulation process. This allows for updating the positions of nodes that are not part of the contour and provide a deformation mesh for each iteration k.

deformation simulators may be employed, however, it is recommended to choose the one that best conforms to the object's behaviour. In this particular paper, a conventional mass-spring-damper-based simulation was used in order to update the mesh.

3   Experiments

This section describes two comparative experiments conducted using an Intel Realsense D435 camera, which provides the RGB frames used in the framework. A light source is aligned with the camera's optical axis to illuminate the texture-less object, allowing for better perception. To evaluate the method's ability to handle sudden deformations, we captured new camera frames at a rate of 0.5 Hz. The objects were manually deformed in a rapid manner, resulting in abrupt changes between consecutive frames. The experiments were conducted on an Intel(R) Core(TM) i7-8565U CPU with 1.99 GHz and 16 GB of RAM and the algorithm was implemented on Matlab R2022b.

Each image sequence was analysed using two methods to show the relevance of our framework. The first method is the one presented in this paper, while the second method involves a mesh update based on an homogeneous contour mapping similar to those used on previous papers such as [12–15]. Homogeneous contour mapping involves sampling both contours with the same number of equidistant points, resulting in a map where contour length variations are assumed to occur uniformly throughout the contour. In contrast, the elastic contour mapping used in our proposed method allows for the identification of cases where specific parts of the contour stretch or contract while others remain unchanged.

Both experiments carried out in this study can be seen in Figures 3 and 4 respectively and in the **attached video** [1]. The figures show, for each experiment, three key frames for both the elastic and the homogeneous contour mapping methods: the initial mesh ($k = 1$), the frame where the abrupt deformation is first detected, and the final state of the mesh after the deformation. The object mesh is displayed in red, while the point matches between consecutive iterations are illustrated as grey lines. For comparison purposes, an additional frame is presented after the sequence where the mesh before the abrupt deformation is overlapped in yellow. Next to the frames, the evolution of the mesh's deformation distribution is presented for both methods. The deformation values are computed as the relative change in length of the mesh's edges with respect to their length at $k = 1$.

3.1   Experiment: red cushion

In this experiment (Fig.3), a red cushion was suddenly stretched horizontally, resulting in the bottom and top segments of the cushion's contour being stretched

---

[1] http://webdiis.unizar.es/%7Eglopez/videos/Cuiral-ZuecoROBOT2023.mp4
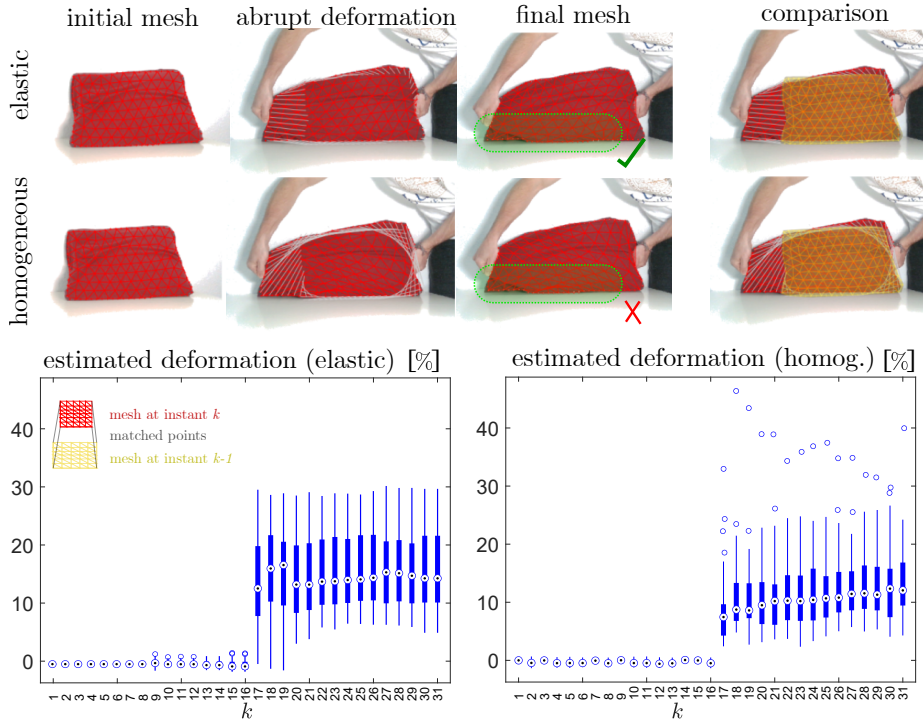
Fig. 3. Elements of the figure are introduced in section 3. This experiment involves the horizontal stretching of a red cushion that causes uneven deformations across its contour. The elastic contour mapping method accurately identified the non-isometric deformation, as evidenced by the horizontal gray lines that represent the point matching on the abrupt deformation frame. In contrast, the homogeneous contour mapping method assumed a uniform contour deformation, resulting in slanted gray lines and an inaccurate mesh deformation estimation. The elastic mapping led to a more uniform distribution of the stretching process, as seen on the bottom left plot. The mesh collapse in the homogeneous mapping case, observed in the green box of the final mesh frame, may have caused the more uneven distribution of deformation distribution seen in the bottom right plot.

while the sides' length remained relatively unchanged. The elastic contour mapping method accurately identified this non-isometric deformation, as demonstrated by the predominantly horizontal gray lines representing the point matching in the abrupt deformation frame of the elastic contour mapping sequence. Conversely, the homogeneous contour mapping method assumed that the deformation was evenly distributed across the contour, resulting in slanted gray lines and a mesh deformation that did not accurately represent the actual process. The analysis of the deformation distributions revealed that the elastic contour mapping method yielded a more uniform distribution of the stretching process. This result was expected since the object was uniformly stretched horizontally. In contrast, the homogeneous contour mapping method produced a more uneven distribution with outliers that reached up to approximately 40%. This may be due to some areas of the mesh collapsing, as highlighted by the green box in the final mesh frame.

3.2   Experiment: blue cloth

This experiment represents an extreme case where a folded sweater's sleeve is suddenly lifted (Fig.4). Although the initial mesh does not represent the actual object configuration, it serves as an illustrative case of the method's performance in cases where the deformation is highly localised in a specific part of the object. The elastic mapping correctly identifies that most of the contour remains unchanged, while the homogeneous mapping estimates a contour point shifting process throughout the bottom of the object. This is well observed in the final mesh frame, where a set of edges on the bottom of the object has been significantly deformed. In the case of the final mesh of elastic contour mapping, the mesh presents less overlap with the object, which is likely due to the need for higher mesh resolution that allows nodes and edges to fit better into significantly deformed object configurations. The deformation distribution plots reveal that the elastic mapping method produced mostly outliers, as expected for the highly localised deformation process, while the homogeneous mapping method showed a more scattered distribution, which contradicts the actual deformation process.

4   Discussion

We proposed a method for estimating the deformation mesh of texture-less objects using visual sensors. The approach builds upon our previously proposed FMM-based contour mapping framework and addresses the more complex task of estimating the object's deformation mesh when sudden deformations occur. Two experiments demonstrate the effectiveness of the method. A limitation is that deformations may occur without affecting the object's contour and thus may not be perceptible by a camera considering the object lacks visual texture.

Future work could involve extending the problem to three dimensions, which would require modifications to account for the additional complexity. Another potential avenue for exploration is using different deformation simulators and
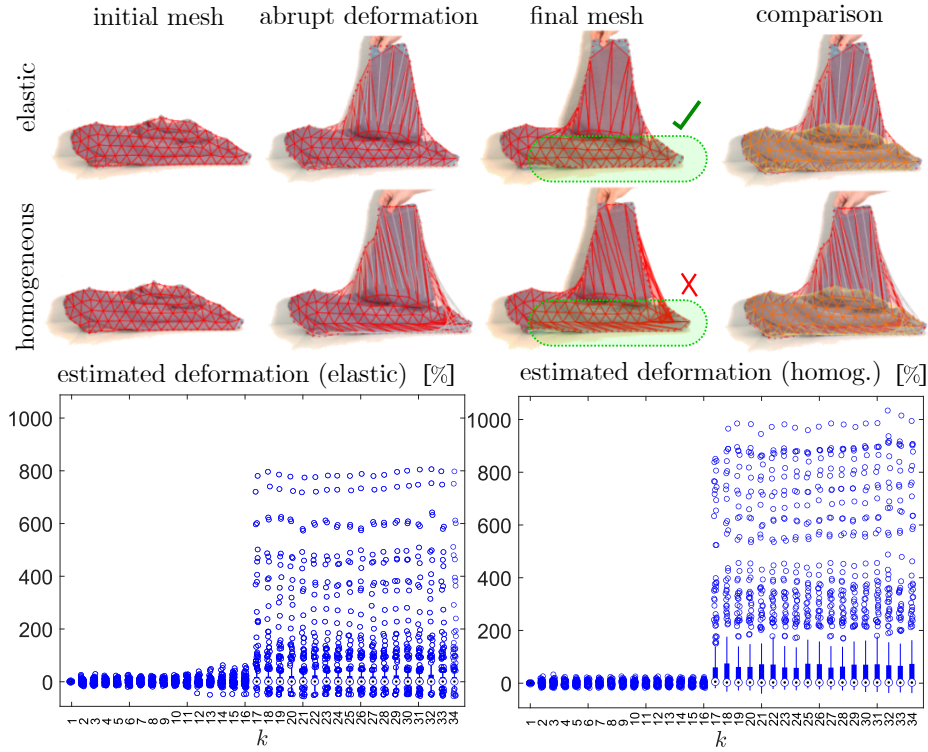
Fig. 4. Elements of the figure introduced in section 3. Comparison of elastic contour mapping and homogeneous mapping on a folded sweater's sleeve lifting experiment. The elastic mapping method correctly identifies that most of the contour remains unchanged while the homogeneous mapping estimates a contour point shifting process throughout the bottom of the object. The final mesh frame of the elastic contour mapping method presents less overlap with the object, likely due to the need for higher mesh resolution in significantly deformed object configurations. As for the deformation distribution plots: the elastic mapping produced mostly outliers, as expected for a highly localised deformation, while the homogeneous approach generated a scattered distribution that contradicts the actual process.

evaluate how they compare in terms of accuracy and computational efficiency. This could involve testing simulators against both simpler and more complex environments and/or objects in order to gain a better understanding of their accuracy, strengths and limitations. Extending the framework to analyse object breakage, e.g., detecting when the object splits in two, would be a valuable addition too.

Acknowledgements

References

1. V. E. Arriola-Rios, P. Guler, F. Ficuciello, D. Kragic, B. Siciliano, and J.L. Wyatt. Modeling of deformable objects for robotic manipulation: A tutorial and review. *Frontiers in Robotics and AI*, 7:82, 2020.
2. R. Herguedas, G. López-Nicolás, R. Aragüés, and C. Sagüés. Survey on multi-robot manipulation of deformable objects. In *24th IEEE International Conference on Emerging Technologies and Factory Automation*, pages 977–984, 2019.
3. J. Sanchez, J.A. Corrales, B.C. Bouzgarrou, and Y. Mezouar. Robotic manipulation and sensing of deformable objects in domestic and industrial applications: a survey. *The International Journal of Robotics Research*, 37(7):688–716, 2018.
4. M. Shetab-Bushehri, M. Aranda, Y. Mezouar, and E. Ozgur. As-rigid-as-possible shape servoing. *IEEE Robotics and Automation Letters*, 7(2):3898–3905, 2022.
5. X. Lin, Y. Wang, Z. Huang, and D. Held. Learning visible connectivity dynamics for cloth smoothing. In *Conference on Robot Learning*, pages 256–266. PMLR, 2022.
6. Z. Cai, L. Wen, Z. Lei, N. Vasconcelos, and S. Z. Li. Robust deformable and occluded object tracking with dynamic graph. *IEEE Transactions on Image Processing*, 23(12):5497–5509, 2014.
7. M. Aranda, J.A. Corrales Ramon, Y. Mezouar, A. Bartoli, and E. Özgür. Monocular visual shape tracking and servoing for isometrically deforming objects. In *IEEE/RSJ International Conference on Intelligent Robots and Systems*, pages 7542–7549, 2020.
8. Ignacio Cuiral-Zueco, Yiannis Karayiannidis, and Gonzalo López-Nicolás. Contour based object-compliant shape control. *IEEE Robotics and Automation Letters*, 8(8):5164–5171, 2023.
9. I. Cuiral-Zueco and G. López-Nicolás. Multi-scale laplacian-based FMM for shape control. In *IEEE/RSJ International Conference on Intelligent Robots and Systems*, pages 3792–3797, 2021.
10. J. A Sethian and A.M. Popovici. 3-D traveltime computation using the fast marching method. *Geophysics*, 64(2):516–523, 1999.
11. P.-O. Persson and G. Strang. A simple mesh generator in matlab. *SIAM review*, 46(2):329–345, 2004.

12. G. López-Nicolás, R. Herguedas, M. Aranda, and Y. Mezouar. Simultaneous shape control and transport with multiple robots. In *IEEE International Conference on Robotic Computing*, pages 218–225, 2020.
13. D. Navarro-Alarcon and Y.H. Liu. Fourier-based shape servoing: a new feedback method to actively deform soft objects into desired 2-D image contours. *IEEE Transactions on Robotics*, 34(1):272–279, 2017.
14. J. Zhu, D. Navarro-Alarcon, R. Passama, and A. Cherubini. Vision-based manipulation of deformable and rigid objects using subspace projections of 2-D contours. *Robotics and Autonomous Systems*, 142:103798, 2021.
15. J. Qi, G. Ma, J. Zhu, P. Zhou, Y. Lyu, H. Zhang, and D. Navarro-Alarcon. Contour moments based manipulation of composite rigid-deformable objects with finite time model estimation and shape/position control. *IEEE/ASME Transactions on Mechatronics*, 2021.